Acta Chemica Scandinavica A 34 (1980) 31 – 42

Conformational Analysis. The Structure and Torsional Potential of 1,3-Butadiene as Studied by Gas Electron Diffraction

KARI KVESETH,[a] RAGNHILD SEIP[a] and DENIS A. KOHL[b]

[a] Department of Chemistry, University of Oslo, Blindern, Oslo 3, Norway and [b] Department of Chemistry, University of Texas at Austin, Austin, Texas 78712, U.S.A.

Gaseous 1,3-butadiene has been studied by electron diffraction at elevated temperatures (25 °C – ~900 °C). The predominant conformation at all temperatures is *anti*, oscillating in a fairly wide potential well. The torsional potential has been expanded by a Fourier series, determined in the least-squares procedure, with coefficients $V_1 = 3.4(4)$, $V_2 = -1.1(5)$, $V_3 = 0.3(6)$ and $V_4 = 0.2(8)$ (kcal mol^{-1}). No evidence for a second stable conformer was obtained, even at the highest temperature studies. However, the presence of an additional potential minimum at least 3.5 kcal mol^{-1} above *anti* and with a low *gauche*/*anti* barrier cannot be excluded.

1,3-Butadiene has been the subject of several studies, by electron diffraction[1-5] as well as by other experimental[6-11] and theoretical[12-15] methods. The planar *anti* form predominates, and to date no conclusive evidence of a second conformer has been given, though both *syn*[10,12] and a distorted *gauche*[3,4,11,13,16] have been suggested for a possible additional conformer.

In an extensive analysis[16] the existing data on butadiene have been evaluated, together with the different assumptions inherent in the various experiments. A potential curve, $V(\phi)$, based upon a four term Fourier series expansion (1)

$$V(\phi) = \sum_{n=1}^{m} \tfrac{1}{2} V_n (1 + \cos n\phi),\ m = 4 \qquad (1)$$

that accounts very well for the combined information, was proposed. This potential curve has a second minimum at ~30° (*anti* corresponds to 180°) and a *gauche-anti* energy difference of 2.66 kcal mol^{-1} (1 kcal = 4.184 kJ). The barrier between *anti* and *gauche* was estimated to 6.03 kcal mol^{-1} at 97.3° and an additional but much lower barrier of 0.09 kcal mol^{-1} was estimated at *syn*. This torsional potential would lead to a high degree of flexibility in the *syn-gauche* region and a fairly rigid molecular model in *anti*. The potential function is presented in Fig. 5 (curve E).

Most substituted 1,3-butadienes[17-22] and analogs[5] have been found in the planar *anti* form, exceptions being those with 1,3-interactions,[19,23,24] where *gauche* forms have been found. In some butadiene analogs containing C=O[25,26] or N=C[27] bonds two conformers are found to coexist, recognized as *anti* and *gauche*. Because of the asymmetry of the *anti*-peak observed in the latter compounds, a model composed of molecular species over a region corresponding to $\pm 2\sigma_\phi$ (σ_ϕ is the root-mean square deviation from *anti*) was introduced in order to describe the large, assumed harmonic, torsional amplitude. From the determined values of ΔH (the conformational enthalpy difference), ϕ_g (the torsional angle in *gauche*) and σ_ϕ, the torsional potential was estimated for these compounds. The potential was expanded in a Fourier series, including the first three terms and assuming a classical Boltzmann probability distribution.

Based upon the observed asymmetry of the $C_1 \cdots C_4$ peak, the scope of this work is to study further the torsional potential and related properties in 1,3-butadiene. In the search for a presumed second conformer, butadiene has been reinvestigated at several temperatures, as high as possible in the electron-diffraction experiment. Due to the high flexibility and low symmetry of this molecule, a study of the internal rotation is more complicated than usually experienced, and it is of interest to

0302-4377/80/010031-12$02.50

examine the applicability of the electron-diffraction method in this connection.

EXPERIMENTAL

The sample of 1,3-butadiene was obtained from Fluka (≥99.8 % pure), and distilled in vacuum. Two sets of electron-diffraction photographs were obtained, set one from the electron-diffraction unit at the University of Texas at Austin,[28] and set two from the Balzers Eldigraph KDG-2 unit[29,30] at the University of Oslo. The experimental conditions are summarized in Table 1. The nozzle applied in the Austin recordings is a hypodermic needle,[28] heated by an electric current. No direct temperature measurement was possible. In the Oslo recordings a modified version of a reaction nozzle, with a solid silver tip and a reaction chamber, was applied. This nozzle system was screened to prevent any light from the hotter parts to reach the plates during exposure. The temperature was measured by a thermocouple at the nozzle tip.

This investigation presents the results of the first study by electron diffraction in Oslo at such high temperatures. The temperature stability of the nozzle system was unknown prior to this study and data were collected only at one nozzle-to-plate distance. Since the torsional properties have been

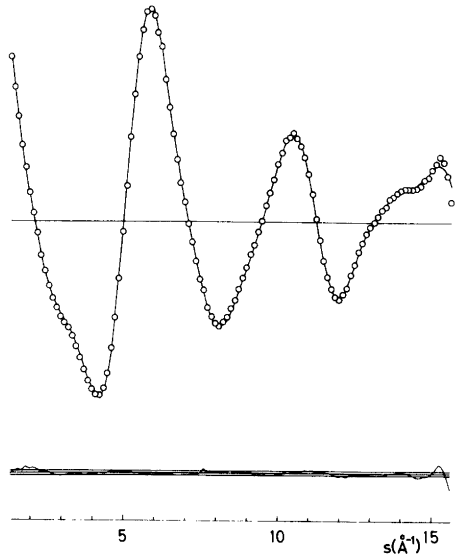

Fig. 1. Intensity curve, Oslo data. The solid curve is theoretical, calculated from the parameters in Table 4, model C. The open circles are experimental values. The difference curve, given below, is experimental minus theoretical. The limits are 3σ, σ being the experimental standard deviation in the observed points.

Table 1. Experimental conditions and photographic plate data.

Austin data

Relative transmittance measured by stepwise scanning, spinning the plate over the full circle at each point.
Nozzle-to-plate distance: 409.24 mm
Range of data (s) : 4.10 – 22.40, $\Delta s = 0.10$ (Å^{-1})

Plate No:						
1	2	3	4	5	6	7
Electron wavelength (Å):[a]						
0.061036	0.061046	0.061057	0.061061	0.061062	0.061062	0.061063
Nozzle heating [current (amp)/voltage (V)]:						
0./0.	6.0/1.3	8.0/1.3	11.9/1.9	11.9/1.9	13.0/2.1	13.0/2.1

Room temp.: 25 °C

Oslo data

Optical densities measured in (x,y)-points by a Joyce-Loebl MK 111 C densitometer, integrated by an interpolation routine over a constant arc.
Nozzle-to-plate distance: 499.26 mm
Range of data (s): 1.375 – 15.625, $\Delta s = 0.125$ (Å^{-1})
No. of plates: 6
Electron wavelength:[b] 0.058630 Å
Nozzle temperature: 500 °C

[a] Some instabilities in the differential voltmeter made it necessary to calibrate the original measurements to the previously obtained geometric parameters of butadiene. [b] As calibrated to benzene.

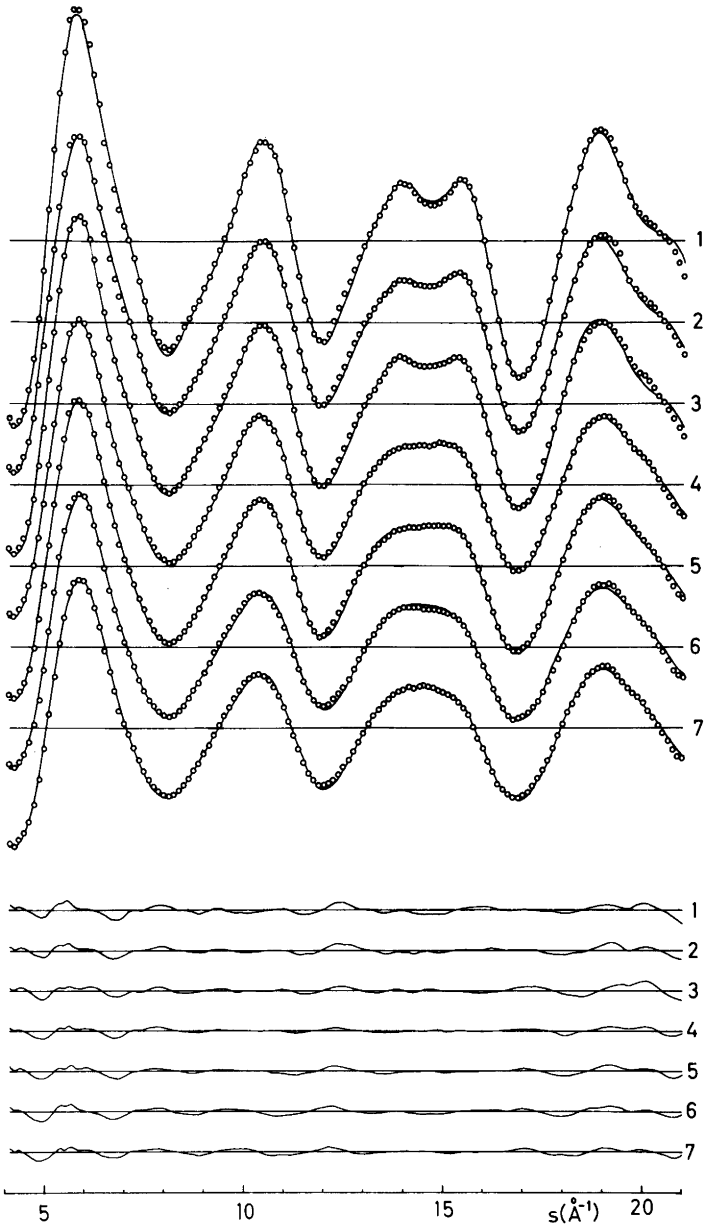

Fig. 2. Intensity curves for each plate, Austin data. The solid curves are theoretical, calculated from the best set of parameters and the Fourier coefficients obtained from refinement C of the Oslo data. The corresponding difference curves are given below.

focused in this study, 50 cm plates were preferred, as the torsional dependant contributions are mainly seen in the intensities at small s-values.

The data were corrected in the usual way,[31] giving one intensity curve for each photographic plate. The intensities were modified with the func-

tion $s/|f_C|^2$. The computer drawn background[32] was subtracted separately from each intensity curve on levelled form. The average for the Oslo data is presented in Fig. 1, and the individual curves from Austin in Fig. 2.

The structural parameters are determined by conventional least-squares refinement on these intensity data.

The theoretical molecular intensities were calculated according to eqn. 11 of Ref. 31. The scattering amplitudes and phase shifts[31,33] were calculated analytically by a program originally written by Yates,[34] using Hartree-Fock-Slater potentials[33] for C and molecular bonded potentials for H.[35]

STRUCTURE ANALYSIS AND REFINEMENT

Radial distribution curves (RD-curves), calculated from the molecular intensities by a Fourier trans-

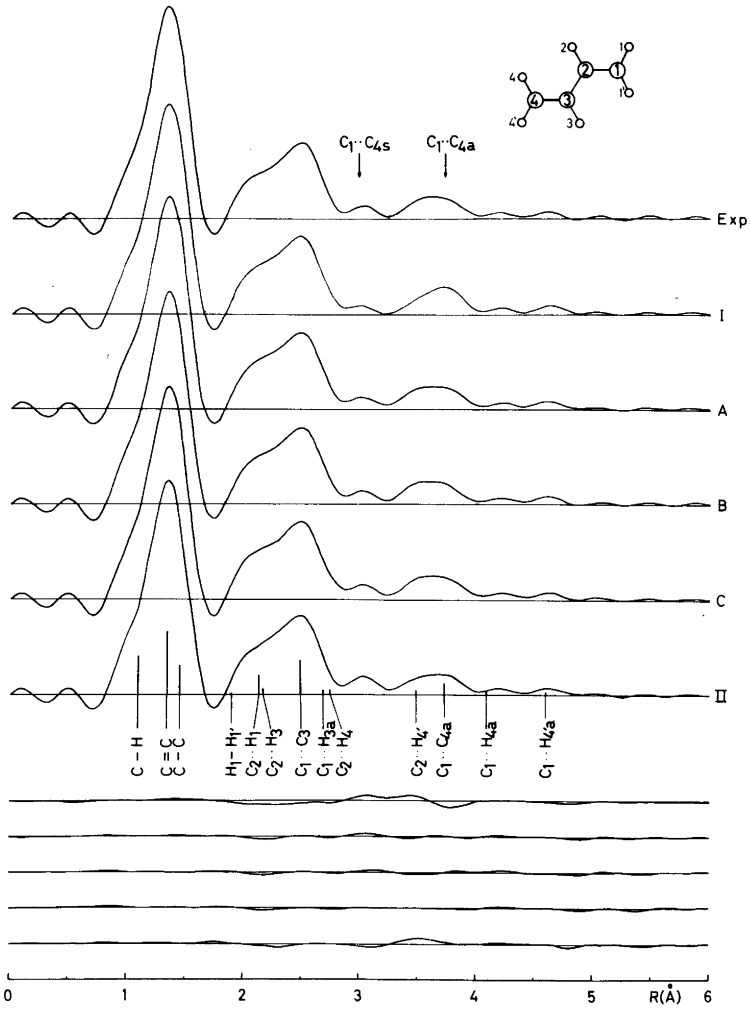

Fig. 3. Radial distribution curves and differences, Oslo data ($B=0.0025$ Å^2). The upper curve is experimental, the curves I, A, B, C and II correspond to different theoretical models: I: 100 % *anti*, A: model A with 55.2 % *anti* and $\phi_g=112.6°$, B: model B with $\sigma_\phi=57.3°$, C: model C with $V_1=3.4$, $V_2=-1.1$, $V_3=0.3$ and $V_4=0.2$ (kcal mol^{-1}) and II: model C with $V_1=0.99$, $V_2=-5.11$, $V_3=1.75$ and $V_4=0.51$ kcal mol^{-1}, potential E[16] of Fig. 5. The differences, given below, are the experimental minus the various theoretical curves.

formation[31] are presented in Figs. 3 and 4. The bond distances contribute to the first two peaks, the major torsional independent distances to the peak complex between 2 and 3 Å. The torsional dependent $C_1 \cdots C_4$ distance in the *anti* region gives rise to the asymmetric peak at 3.7 Å.

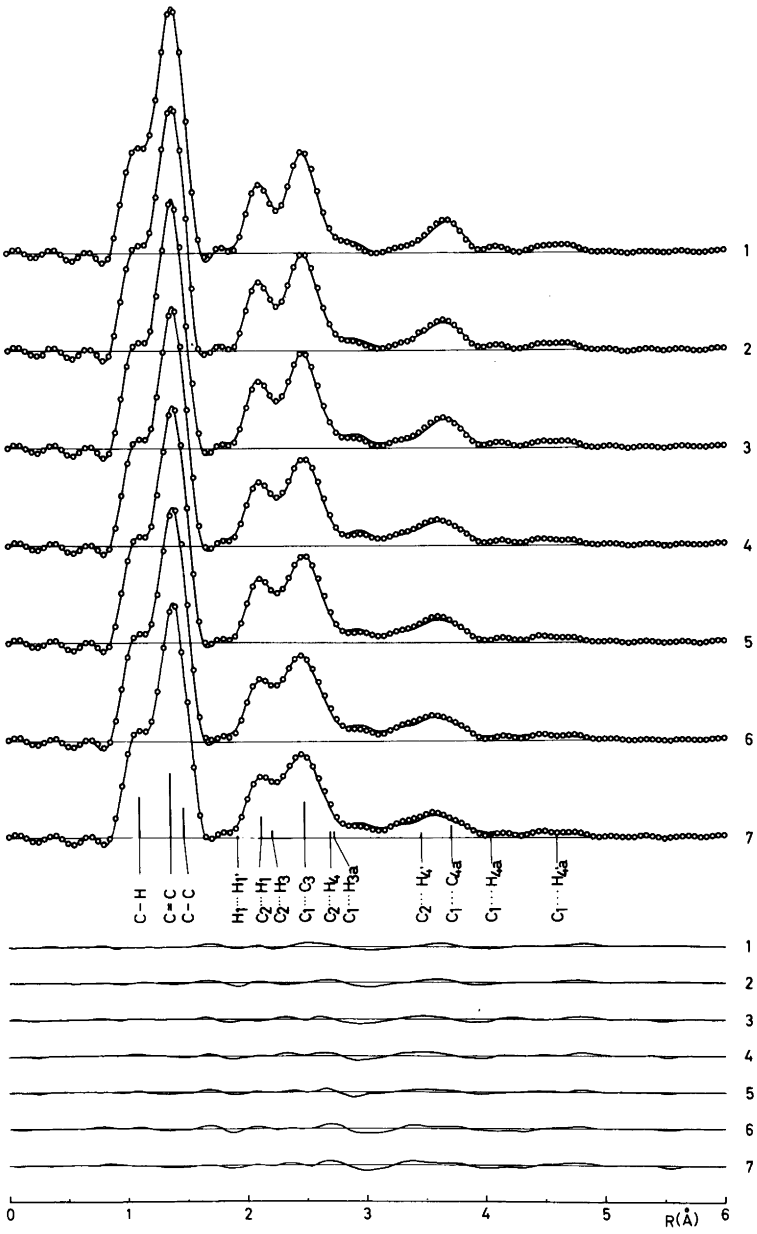

Fig. 4. Radial distribution curves for each plate and differences, Austin data ($B = 0.0025$ Å^2). The open circles are the experimental values, the solid curves correspond to the theoretical curves with the Fourier coefficients obtained from refinement C of the Oslo data (Table 4, line II). The corresponding differences are given below.

The area and shape of this outer peak complex is dependent of the torsional distribution about the C–C axis.

The following parameters were chosen as independent structural parameters: The three bond distances, r(C–C), r(C=C) and r(C–H) (all C–H-distances were assumed to be identical), the angles $\angle$CCC, $\angle C_2C_1H_1$, $\angle C_1C_2H_2$ and the torsional angle about the C–C axis, ϕ. ϕ is defined as 180° in *anti*, where the molecule is assumed to be planar.

The C–C torsional independent parameters were assumed to be identical for all values of ϕ. The torsional distribution is primarily determined from the torsional dependent $r(C_1\cdots C_4)$ and to a smaller extent by $r(C_1\cdots H_3)$, $r(C_1\cdots H_4)$ and $r(C_1\cdots H_{4'})$.

The data were analyzed by applying three different models. In approach A the molecule is assumed to exist as a conformational mixture of *anti* and *syn* or *gauche*. Both conformations are described as rather rigid molecular species each characterized by appropriate root-mean-square vibrational amplitudes (u-values).

The two other models represent more flexible molecular species. In model B the torsional potential, $V(\phi)$, is assumed to be harmonic, but with a wide potential well in *anti*. The torsional distribution is described by the root-mean-square angular

Table 2. Valence force constants.

Stretch (mdyn Å^{-1})		Interaction	
f_{C-C}	6.07	$f_{C=C,C_2C_1H_1}$	0.16
$f_{C=C}$	8.15	$f_{C=C,HCH}$	−0.05
$f_{C_1-H_1}$	5.07	$f_{C-C,C_3C_2H_2}$	0.12
$f_{C_2-H_2}$	5.01	$f_{C-C,C_1C_2H_2}$	−0.24
		$f_{C_2C_1H_1,HCH}$	−0.02
Bend (mdyn Å rad^{-2})		$f_{C_1C_2H_2,C_3C_2H_2}$	0.08
$f_{C_2C_1H_1}$	0.52	$f_{CCC,C_3C_2H_2}$	0.19
f_{HCH}	0.37	$f_{C=C,C-H}$	0.10
$f_{C_3C_2C_2}$	0.62	$f_{C=C,C-C}$	0.58
f_{CCC}	0.99	$f_{\tau,C-C,o.o.p.C_1}$	−0.03
$f_{o.o.p.C_2}$	0.23	$f_{\tau,C=C,o.o.p.C_1}$	0.09
$f_{o.o.p.C_1}$	0.30		
Torsion (mdyn Å rad^{-2})			
$(f_{\tau,C-C}$	0.102)[a]		
$f_{\tau,C=C}$	0.642		

[a] From the electron diffraction data $f_{\tau,C-C} = 0.02$ mdyn Å rad^{-2}.

Table 3. Vibrational amplitudes, u(Å), as calculated from the valence force field.

Distance[a] type	r(Å)	u(Å) 25 °C	200 °C	500 °C	600 °C	900 °C
C–C	1.46	0.046	0.047	0.051	0.053	0.058
C=C	1.34	0.043	0.043	0.046	0.047	0.051
C–H	1.10	0.077	0.077	0.078	0.078	0.079
$C_1\cdots C_3$	2.48	0.065	0.072	0.086	0.090	0.103
$C_2\cdots H_3$	2.18	0.103	0.106	0.114	0.118	0.128
$C_2\cdots H_1$	2.13	0.099	0.102	0.108	0.111	0.120
$H_1\cdots H_{1'}$	1.89	0.123	0.124	0.128	0.130	0.137
$C_2\cdots H_{4'}$	3.47	0.098	0.102	0.111	0.114	0.124
$C_2\cdots H_4$	2.73	0.144	0.157	0.183	0.191	0.216
$H_2\cdots H_{1'}$	3.11	0.121	0.122	0.127	0.129	0.137
$H_2\cdots H_1$	2.47	0.161	0.166	0.182	0.188	0.207
$C_1\cdots C_4$	3.70	0.066	0.074	0.088	0.093	0.106
$C_1\cdots H_3$	2.68	0.142	0.155	0.181	0.189	0.213
$H_2\cdots H_3$	3.13	0.126	0.128	0.134	0.137	0.146
$C_1\cdots H_{4'}$	4.60	0.110	0.117	0.131	0.136	0.150
$C_1\cdots H_4$	4.07	0.143	0.156	0.181	0.189	0.214
$H_3\cdots H_1$	3.78	0.158	0.169	0.192	0.200	0.222
$H_3\cdots H_{1'}$	2.47	0.211	0.232	0.274	0.287	0.325
$H_1\cdots H_{4'}$	5.57	0.132	0.136	0.147	0.151	0.164
$H_1\cdots H_4$	4.78	0.188	0.205	0.239	0.250	0.281
$H_{1'}\cdots H_4$	4.67	0.169	0.180	0.204	0.212	0.237

[a] For numbering of atoms see Fig. 3.

Table 4. Molecular parameters, distances (r_a) and vibrational amplitudes (u) in Å, angles ($\angle_a$) in degrees, Fourier coefficients (V_n) in kcal mol^{-1}, and estimated correlation coefficients (ρ) larger than 0.5. Standard deviations (1σ) in parentheses. $R_2 = (\sum w\Delta^2/\sum wI^2)^{\frac{1}{2}} \cdot 100$.[38,39]

a. Oslo data: 500 °C.

Model	A	B	C
r(C−C)	1.467(2)	1.467(2)	1.468(2)
r(C=C)	1.349(1)	1.349(1)	1.348(1)
r(C−H)	1.108(1)	1.108(1)	1.107(1)
∠CCC	124.4(1)	124.4(1)	124.3(1)
$\angle C_1C_2H_2$	120.9(4)	120.9(4)	120.7(3)
ϕ_g	112.6(44)		
n_a(%)	55.2(46)		
σ_ϕ		57.3(24)	
V_1			3.4(4)
V_2			−1.1(5)
V_3			0.3(6)
V_4			0.2(8)
R_2(%)[a]	3.79	3.68	3.30
$\rho(r(C=C), r(C-H))$	0.68	0.66	0.67
$\rho(V_1, V_2)$			−0.75
$\rho(V_3, V_4)$			−0.69

b. Austin data.

Curve No:	1	2	3	4	5	6	7
Estim. temp. (°C)	25	200		600		900	
I: model B							
σ_ϕ	23.2(21)	33.2(22)	39.3(22)	56.0(23)	54.8(29)	51.0(33)	55.2(30)
R_2(%)	4.86	4.73	4.68	3.61	4.44	4.95	4.06
II: model C ($V_1 - V_4$ as above)							
R_2(%)	4.81	4.86	5.04	4.37	5.19	6.16	5.44
III: model C ($V_3 - V_4$ as above)							
V_1	9.6(199)	7.5(39)	5.6(20)	7.6(13)	7.9(17)	13.1(36)	11.3(24)
V_2	1.0(62)	0.8(15)	0.5(9)	2.1(7)	2.1(9)	3.9(18)	3.8(13)
R_2(%)	4.77	4.67	4.89	3.75	4.58	4.98	4.27

[a] The R_2-factors for models I and II (Fig. 3) are 6.78 and 4.28 %, respectively.

amplitude, σ_ϕ, and integrated over $\pm 2.5\sigma_\phi$. σ_ϕ is determined in the least-squares procedure. In this case σ_ϕ and the torsional force constant, f_τ, is related through eqn. 2.

$$f_\tau = RT/\sigma_\phi^2 \quad (2)$$

In model C the torsional potential is expressed by a terminated Fourier series expansion (eqn. 1), including the first four terms, previously[10,16] found to be necessary to describe appropriately the observed frequencies. The torsional distribution is integrated over the whole ϕ-region. In this case f_τ may be defined at the minima, ϕ_m, of the potential curve as

$$f_{\tau,\phi_m} = \partial^2(V(\phi))/\partial^2(\phi)_{\phi_m} \quad (3)$$

A normal coordinate analysis[36] has been carried out to determine a valence force field (Table 2) in agreement with the observed frequencies.[37] The u-values calculated from the normal coordinates[38] are presented in Table 3. These values agree excellently with those previously presented.[5,37]

In the least-squares refinements only diagonal elements in the weight matrix[39,40] were included.

The determined structural parameters are presented in Table 4. The obtained standard deviations (1σ), including the uncertainty of 0.1 % in the wavelength, are given in parentheses.

RESULTS AND DISCUSSION

Due to the *s*-scale uncertainties in the Austin material these data are primarily used in the studies of the torsional potential. The structural data presented in Table 4 refer to the set of data obtained in Oslo.

The obtained geometry parameters agree excellently with those determined previously.[3,5] Due to the comparatively limited *s*-range of the applied data, the choice of start-parameters interferes severely with the background.

It was not possible to distinguish between the two CCH angles, $\angle C_1C_2H_2$ and $\angle C_2C_1H_1$, and the average value has been determined. All *u*-values have been kept at the calculated values in the various least-squares refinements.

The RD-curves given in Fig. 3 reveal that both 100 % *anti* (rigid model, curve I) as well as a model (curve II) oscillating in the spectroscopically proposed potential[16] (curve E, Fig. 5) can be rejected. The three molecular models A–C describe satisfactorily the experimental data. Although the lower R_2 factor gives a slight preference for model C, based on these data alone, we cannot discriminate between the applied models.

The obtained torsional angle (112.6°) for the *gauche* conformation (model A) is significantly larger than 80–85° as obtained at 390 °C,[4] where

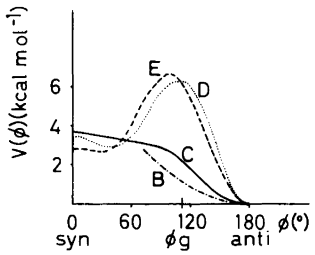

Fig. 5. Torsional potentials. B: as obtained from σ_ϕ, Oslo data, model B. (eq. 2) C: as obtained from the Fourier coefficients, Oslo data, model C. D: as obtained from an *ab initio* calculation with optimized geometry, extrapolated from the four points obtained by Skaarup *et al.*[14] E: as obtained from the Fourier coefficients given by Bock *et al.*[16]

80 % *anti* was estimated. In model A the *u*-values have been calculated from spectroscopic data for both conformers, and the difference in the obtained ϕ_g values may reflect that different assumptions about the torsional dependent *u*-values have been applied. Keeping the torsional dependent *u*-values constant at the value of *anti*, an increased *anti* fraction and a decrease in the torsional angle of the same order of magnitude were found.

The obtained torsional angle seems indeed unreasonable. Such a large angle rather indicates that the torsional potential is very wide, and that the unexpected value is the result of the least-squares refinement of an inadequate model.[41]

To illustrate this statement a model with two rigid conformers was fitted by the least-squares method to a theoretical curve calculated from model B ($\sigma_\phi = 57°$). An excellent agreement was obtained with 64(1) % *anti* and $\phi_g = 109(1)°$. This result may serve as a warning which concerns all conformational studies. The least-squares method will always give the best fit of any model chosen to describe the molecular system. The evaluation of the obtained results has to be based on chemical intuition and the analogy with related compounds.

In order to describe the torsional behaviour of butadiene, even in the vicinity of *anti*, a more flexible model as B and/or C has to be introduced.

The resulting torsional potentials are presented in Fig. 5. There are two striking differences between the obtained potentials B and C on one side, compared with those obtained from *ab initio* calculations[13,14] (D) or spectroscopically[16] (E) on the other side. The minimum of potentials B and C are much broader and the torsional energy increases steadily on going from *anti* to *syn*, producing no second minimum in the torsional potential. Ac-

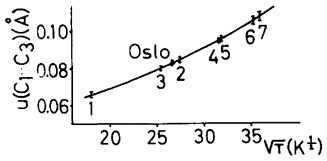

Fig. 6. $u(C_1\cdots C_3)$ given as functions of $T^{\frac{1}{2}}$. The corresponding refined *u*-values are given the appropriate curve No., the vertical lines (1σ) indicate the uncertainty. Temperature measurements from the $u(C_1\cdots C_3)$ curve; Oslo data: 435 °C (nozzle temp.: 500 °C), Austin data; 1; 51 °C (nozzle temp.: 25 °C), 2; 477 °C, 3; 372 °C, 4; 725 °C, 5; 738 °C, 6; 970 °C, 7; 1000 °C.

cording to eqn. 2 potential B corresponds to a torsional force constant $f_\tau^B = 0.01$ mdyn Å rad^{-2}. From eqn. 3 $f_\tau^C = 0.02$ mdyn Å rad^{-2} is obtained for potential C. The potentials D and E correspond to $f_\tau^D = 0.15$ and $f_\tau^E = 0.10$ mdyn Å rad^{-2}, respectively.

Since the Austin data cover a large temperature interval, these data may be used for further analysis of the two approaches (B and C). In this case the higher temperatures were not measured directly, but have been estimated from the temperature dependency of $u(C_1 \cdots C_3)$ by plotting the spectroscopically obtained u-values as a function of $T^{\frac{1}{2}}$ (Fig. 6).

The temperatures thus determined for the Oslo data, presented in this figure as well, and for the Austin recording at 25 °C (curve 1) agree satisfactorily with the nozzle temperatures, and reveal that this procedure should give the temperatures with reasonable accuracy.

The seven Austin recordings are grouped as the experimental conditions would predict. However, applying the obtained temperatures (Fig. 6) directly revealed some discrepancies in the torsional independent part of the RD-curves, and the temperatures (Table 4) used in the final treatment of these data were arrived at in a cyclic manner by improving the fit to the torsional independent part of the experimental RD-curves. Except for the lower temperature obtained for curves 2 and 3, the final values are in good agreement with those obtained from the refined $u(C_1 \cdots C_3)$ values. A similar temperature analysis based on the refined $u(C_2 \cdots H_1)$ gave the same tendencies. But the results appeared to be less reliable, due to the much slower variation of $u(C_2 \cdots H_1)$ with $T^{\frac{1}{2}}$ and the comparatively lower contribution from this distance to the total intensity.

Using model B for the Austin data revealed that in order to satisfactorily account for the asymmetry in the *anti* peak, the obtained σ_ϕ-values increase in such a way that the model is inadequate for a quantitative description of $V(\phi)$. This is demonstrated by the subsequent decrease of the obtained f_τ-values (eqn. 2) with increasing temperature. Since this argument is based on the knowledge of the temperature, the inconsistency may also be demonstrated if we assume that $f_\tau^B = 0.01$ mdyn Å rad^{-2} (the Oslo value) is a reasonable value. Thus combined with the obtained Austin σ_ϕ-values through eqn. 2 this f_τ^B-value would lead to unacceptable temperatures (the recording at room temperature for example would correspond to −142 °C). Thus based on the Austin data model B may be rejected, which leave[3] us with model C as the only acceptable model. However, the Austin σ_ϕ value at room temperature corresponds to $f_\tau = 0.02$ mdyn Å rad^{-2}, identical to the value obtained from the Fourier expanded potential (C) of the Oslo data. This implies that at comparatively low temperatures model B will satisfactorily describe the torsional distance distribution about *anti*. But at higher temperatures model C must be used for an adequate description of the torsional distribution.

The consistency of the obtained Fourier expanded potential (model C) is quite reasonable for all seven Austin curves (Fig. 4, Table 4, line II). The obtained RD-difference curves are still somewhat large, even when taking into account that these curves are individual recordings, whereas the Oslo data are averaged over 6 plates.

In an attempt to determine the four Fourier coefficients from the Austin data as well, only V_1 and V_2 could be refined. V_3 and V_4 were kept constant at the values obtained from the Oslo data, which, of course, limits the freedom of the obtainable V_1 and V_2 values. Although the obtained values (Table 4, line III, Fig. 7) are not significantly different from those in column C, Oslo data, the large standard deviations taken into account, the most striking difference is the fact that the Austin data lead to larger V_1 and consequently larger and opposite in sign V_2-terms. As the curves in Fig. 7 indicate, the effect of the increased size of V_1 and V_2 mainly influences the torsional potential near *syn*, but the resulting potentials about *anti* are in all cases quite open and similar in magnitude to that in curve C.

This apparent inconsistency in the *syn*-region mainly reflects that too detailed information is

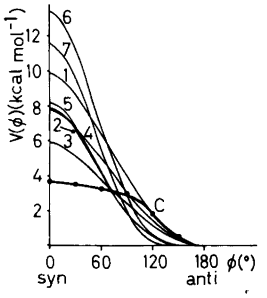

Fig. 7. Torsional potentials as obtained from refinements on the Austin data.

sought. But it may also indicate that including only the first four Fourier coefficients is not sufficient to describe the torsional potential in the whole ϕ-region. Higher order terms should be included in order to assure a sufficient flexibility, so that at elevated temperatures where the relative contribution from the small ϕ-angles plays a more important role, this contribution may be obtained correctly together with the appropriate contribution from the *anti* region.

The large standard deviations obtained for $V_1 - V_4$ (Table 4, Oslo data), together with the positive V_2-values determined from the Austin data, indicate that in order to reproduce the electron-diffraction data a potential function defined in the *anti* region including only the V_1-term is sufficiently accurate. However, since the previous studies of the torsional potential of butadiene[16] on the contrary have given a potential function dominated by the V_2-term (in order to produce a second potential minimum), with not negligible V_1 and V_3-terms, the flexibility of a four term expansion series was preferred in this study.

In models B and C it has been assumed that the torsional motion may be separated from the low out-of-plane bending vibrations. The *u*-framework values have been treated as torsional independent (given the values calculated in *anti*). As illustrated by Fig. 8 this assumption is quite good about 90° out of *anti*. Including the angular dependency for the *u*-framework functions between 90° and *syn*

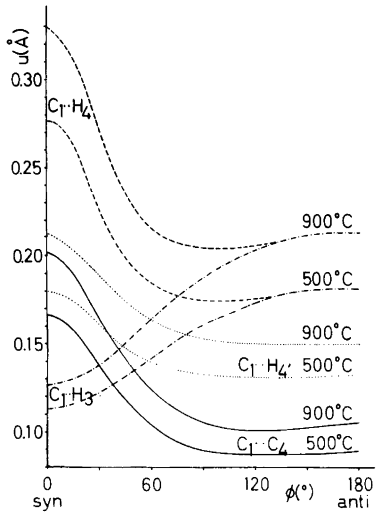

Fig. 8. *u*-framework as obtained from the applied force field (Table 2) as a function of ϕ.

produced in the Oslo data a slightly higher (0.3 kcal mol^{-1}) barrier in *syn*, and an indication of a second minimum at $\phi = 55°$, 2.6 kcal mol^{-1} above *anti*. In the high temperature cases (curves 6 and 7, Austin) introducing $u^{fr}(\phi)$ resulted in slightly smaller values for V_1 and V_2. But within the present level of accuracy, the result is not significantly different from that given in column C, Table 4. Due to the large standard deviations and the uncertainties regarded the separability of the torsional motion and the possibilities of geometric relaxation, it was felt appropriate at this stage to present the results obtained when *u*-framework is treated as torsional independent. The inherent model assumptions together with the very low contributions from molecular species with angles smaller than 70°, indeed make the obtained potentials very uncertain in the *syn* region. But based on this study we may conclude that the torsional potential about *anti* seems much more open than predicted from spectroscopic studies.[10,16]

A torsional force constant of 0.02(5) mdyn Å rad^{-2} corresponds to a torsional frequency of 70(60) cm^{-1}, about half, although formally not significantly different, of what has been assigned to this mode (163 cm^{-1}).[37] The far-IR spectrum of butadiene was reinvestigated, but revealed no evidence for a peak in this region at ambient temperature. A considerable lowering of the torsional frequency may be obtained in the related molecules 1,1-difluoro-[21] and 2-fluoro-1,3-butadiene[22] if calculated from the inertial defects[42] instead of applying the usual relative intensity approach (59 *versus* 103 and 93 *versus* 156 (cm^{-1}), respectively). The extremely low torsional frequency observed in 1,1-difluoro-3-methyl-1,3-butadiene[43] (56 from the inertial defect and 35(cm^{-1}) from relative intensities) supports the idea of a lower torsional frequency in butadiene as well. However, the rather thorough spectroscopic studies[10,44,45] of this mode in *anti* indicate that the torsional potential as estimated from the electron-diffraction data is too wide at the bottom. As reflected in the larger R_2-factor obtained when the spectroscopic potential (Fig. 5, curve E) is introduced compared with that of model C [4.28 *versus* 3.30 (%)] a potential with an *anti/gauche* barrier in the order of 6 kcal mol^{-1} at $\phi = 97°$ is very unlikely. A steady increase in the torsional potential as going from *anti* to *syn* is suggested, although it is emphasized that barriers of this order determined by the electron diffraction method indeed are uncertain.[46]

CONCLUSION

The main conclusions of this investigation are:

(a) The torsional distribution of molecular species about *anti* cannot be assumed to be harmonic above room temperature.

(b) The torsional potential about *anti* as determined from the electron-diffraction data seems to disagree with the spectroscopic results. Firstly the potential well in *anti* is found to be more open, secondly an *anti/gauche* barrier at 97° in the order of 6 kcal mol^{-1} has not been reproduced.

(c) No second conformer has been observed, even at the highest temperatures (900 °C). However, the presence of a second stable form in the *syn/gauche* region at least 3.5 kcal mol^{-1} (less than 10 %) cannot be ruled out.

Acknowledgements. The cooperation with Dr. Z. Smith and other members of the ED-group at the University of Texas at Austin is in particular acknowledged. Without the hospitality and eagerness of this group, the high temperature recordings would not have been possible. Mrs. S. Gundersen is acknowledged for photometering the Oslo-plates as well as running the first computer programs, and Mr. H. V. Volden for drawing the figures. Dr. H. Møllendal should be thanked for introducing us to the inertial defect in MW and Prof. P. Klæboe for recording the far-IR spectrum. We are also grateful to Prof. O. Bastiansen for his interest in this work and for many helpful discussions. Financial support by NAVF, for K. K.'s visit at the University of Texas as well as the grant she has received to complete this work is gratefully acknowledged.

REFERENCES

1. Bastiansen, O. *Om noen av de forhold som hindrer den fri dreibarhet om en enkeltbinding*, A. Garnæs bokstrykkeri, Bergen 1948.
2. Almenningen, A., Bastiansen, O. and Trætteberg, M. *Acta Chem. Scand. 12* (1958) 1221.
3. Haugen, W. and Trætteberg, M. In Andersen, P., Bastiansen, O. and Furberg, S., Eds., *Selected Topics in Structural Chemistry*, Universitetsforlaget, Oslo 1962, p. 113.
4. Trætteberg, M. *Private communication.*
5. Kuchitsu, K., Fukuyama, T. and Morino, Y. *J. Mol. Struct. 1* (1967–68) 463.
6. Aston, J. G., Szasz, G., Wooley, H. W. and Brickwedde, F. G. *J. Chem. Phys. 14* (1946) 67.
7. Lipnick, R. L. and Garbisch, E. W., Jr. *J. Am. Chem. Soc. 95* (1973) 6370.
8. Lide, D. R., Jr. and Jen, M. *J. Chem. Phys. 40* (1964) 252.
9. Fateley, W. G., Harris, R. K., Miller, F. A. and Witkowski, R. E. *Spectrochim. Acta 21* (1965) 231.
10. Carreira, L. A. *J. Chem. Phys. 62* (1975) 3851.
11. Durig, J. R., Bucy, W. E. and Cole, A. R. H. *Can. J. Phys. 53* (1975) 1832.
12. Radom, L. and Pople, J. A. *J. Am. Chem. Soc. 92* (1970) 4786.
13. Skancke, P. N. and Boggs, J. E. *J. Mol. Struct. 16* (1973) 179.
14. Skaarup, S., Boggs, J. E. and Skancke, P. N. *Tetrahedron 32* (1976) 1179.
15. Altmann, J. A. and Reynolds, W. F. *J. Mol. Struct. 36* (1977) 149.
16. Bock, C. W., George, P., Trachtman, M. and Zanger, M. *J. Chem. Soc. Perkin Trans. 2* (1979) 26.
17. Vilkov, L. V. and Sadova, N. I. *Zh. Strukt. Khim. 8* (1967) 398.
18. Aten, C. F., Hedberg, L. and Hedberg, K. *J. Am. Chem. Soc. 90* (1968) 2463.
19. Trætteberg, M. *Acta Chem. Scand. 24* (1970) 2295.
20. Hagen, K. and Hedberg, K. *J. Am. Chem. Soc. 95* (1973) 8266.
21. Beaudet, R. A. *J. Chem. Phys. 42* (1965) 3758.
22. Lide, D. R. *J. Chem. Phys. 37* (1962) 2074.
23. Cyang, C. H., Andreassen, A. L. and Bauer, S. H. *J. Org. Chem. 36* (1971) 920.
24. Gundersen, G. *J. Am. Chem. Soc. 97* (1975) 6342.
25. Hagen, K. and Hedberg, K. *J. Am. Chem. Soc. 95* (1973) 1003.
26. Hagen, K. and Hedberg, K. *J. Am. Chem. Soc. 95* (1973) 4796.
27. Hagen, K., Bondybey, V. and Hedberg, K. *J. Am. Chem. Soc. 99* (1977) 1365.
28. Leggett, T. L., Kennerly, R. E. and Kohl, D. A. *J. Chem. Phys. 60* (1974) 3264.
29. Zeil, W., Haase, J. and Wegmann, L. *Z. Instrumentenkd. 74* (1966) 84.
30. Bastiansen, O., Graber, R. and Wegmann, L. *Balzers High Vacuum Report 25* (1969) 1.
31. a. Andersen, B., Seip, H. M., Strand, T. G. and Stølevik, R. *Acta Chem. Scand. 23* (1969) 3224; b. Gundersen, G. *The Norwegian Electron Diffraction Group Annual Report*, NAVF (1977) 10.
32. a. Hedberg, L. *5th Austin Symposium on Gas Phase Molecular Structure 37* (1974); b. Gundersen, G. and Samdal, S. *The Norwegian Electron Diffraction Group Annual Report, NAVF* (1976) 9.
33. Strand, T. G. and Bonham, R. A. *J. Chem. Phys. 40* (1964) 1686.
34. Yates, A. C. *Comput. Phys. Commun. 2* (1971) 175.

35. Stewart, R. F., Davidson, E. R. and Simpson, W. T. *J. Chem. Phys. 42* (1965) 3175.
36. Gwinn, W. D. *J. Chem. Phys. 55* (1971) 477.
37. Panchenko, Yu. N. *Spectrochim. Acta Part A 31* (1975) 1201.
38. Stølevik, R., Seip, H. M. and Cyvin, S. J. *Chem. Phys. Lett. 15* (1972) 263.
39. Seip, H. M. and Stølevik, R. In Cyvin, S. J., Ed., *Molecular Structure and Vibrations*, Elsevier, Amsterdam 1972.
40. Seip, H. M., Strand, T. G. and Stølevik, R. *Chem. Phys. Lett. 3* (1969) 617.
41. Kveseth, K. *Acta Chem. Scand. A 33* (1979) 453.
42. Gordy, W. and Cook, R. L. *Microwave Molecular Spectra*, Interscience, New York 1970, p. 531.
43. Huang, Y. S. and Beaudet, R. A. *J. Mol. Spectrosc. 34* (1970) 1.
44. Cole, A. R. H., Green, A. A. and Osborne, G. A. *J. Mol. Spectrosc. 48* (1973) 212.
45. Hills, G. W. and Jones, W. J. *J. Chem. Soc. Faraday Trans. 2, 71* (1975) 827.
46. Bastiansen, O., Kveseth, K. and Møllendal, H. *Curr. Chem. Top. 81* (1979) 99.

Received May 25, 1979.